Title
Phase Diagram for Sodium Clusters

Authors
Maiti, A.
Falicov, L.M.

Publication Date
1991-10-01

LBL-31400
Preprint

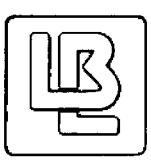

Lawrence Berkeley Laboratory
UNIVERSITY OF CALIFORNIA

Materials & Chemical Sciences Division

Submitted to Physical Review Letters

Phase Diagram for Sodium Clusters

A. Maiti and L.M. Falicov

October 1991

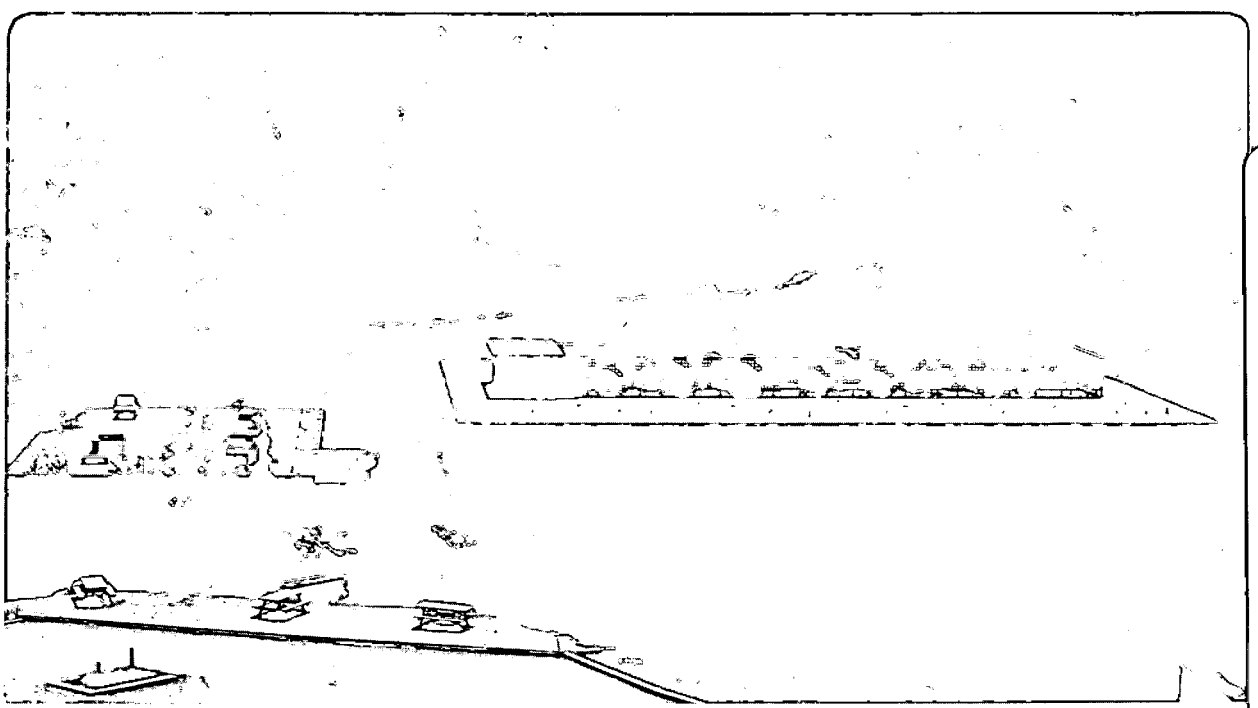

Prepared for the U.S. Department of Energy under Contract Number DE-AC03-76SF00098

DISCLAIMER

LBL-31400

PHASE DIAGRAM FOR SODIUM CLUSTERS*

Amitesh Maiti and L. M. Falicov

Department of Physics
University of California
Berkeley, CA 94720

and

Materials Sciences Division
Lawrence Berkeley Laboratory
Berkeley, CA 94720

October 1991

---

*This work was supported in part by the Director, Office of Energy Research, Office of Basic Energy Sciences, Materials Sciences Division of the U. S. Department of Energy under Contract No. DE-AC03-76SF00098.

Version dated October 15, 1991

Phase Diagram for Sodium Clusters

Amitesh Maiti

and

L. M. Falicov

Department of Physics,
University of California,
Berkeley, California, 94720

and

Materials Sciences Division,
Lawrence Berkeley Laboratory,
Berkeley, California, 94720

Abstract

A temperature-size (T - N) phase diagram is derived for Na clusters of up to $N \sim 1000$ atoms. It is based on first-order pseudopotential calculations, and the Lindemann criterion for melting. It contains three regions of stability: (1) a liquid (jellium) phase at temperatures above the melting line $T_M(N)$; (2) a phase related to the body-centered-cubic structure at temperatures below the melting line; and (3) a close-packed structure at very low temperatures and sufficiently large N. The melting line drops to $T_M(N) = 0$ for $N < 65$. The phase diagram reduces asymptotically to the known phases of Na as $N \rightarrow \infty$, including the known martensitic transformation at $T \approx 5$ K.

Ever since the discovery of "electronic" magic numbers[1] in the abundance spectrum of small Na clusters, metallic-cluster physics has become an active topic of research. A compelling stimulus throughout has been to understand, both theoretically and experimentally[2], how the bulk crystalline solid structure evolves from the growing cluster aggregates. Data on alkali metal clusters up to a size of several thousand have recently been reported[3-5]. The accepted picture, emerging from these experiments, has been the following: for sizes up to around a thousand the most stable clusters are of quantal origin[3,4], *i.e.*, belong to "some" series of electronic magic numbers, whereas for sizes between ~ 1,500 - 22,000 the most stable clusters correspond to geometrically (icosahedral or cuboctahedral) closed shell of atoms[5]. Despite the lack of good resolution in the abundance spectrum for larger clusters, the results are believed to support a theoretical picture, based on (uniform[6,7] and non-uniform[8]) self-consistent jellium model (SJBM) calculations, in which a bunching of electronic shells[9] or supershells[10] occur. Although there exist molecular dynamics (or similar) calculations[11-16] that incorporate the position of the ions in the clusters explicitly, these are computationally limited to small clusters ($N < 50$ in most cases), and are unable to treat clusters of several-hundred size, which are to be addressed primarily in this letter. In an earlier contribution[17] a pseudopotential calculation was performed on a simplified model of spherical clusters, in order to shed light on the ionic structure of the clusters and, in particular, to look for a possible transition of cluster stability from the "electronic" magic-number structures at smaller

sizes to geometrically closed, lattice-induced structures for larger sizes. That calculation, for $T = 0$ and Na clusters up to $N \sim 200$, showed a clear transition, at $N \sim 100$ from electronic to lattice-induced magic numbers. Of the two competing structures, *fcc* and *bcc*, considered for the lattice-induced stable clusters, the *fcc* (close packed) is always more stable.

The present contribution extends the calculation of Ref. 17 to larger clusters ($200 < N < 800$), and finite temperatures. It confirms the earlier results at T=0: *fcc* lattice-induced (close-packed) clusters **are** the stable phase in this size regime. For finite temperatures a new picture emerges: at "high temperatures" the experimentally observed stable clusters are to be interpreted as solely caused by thermal melting of the clusters. Jellium becomes an appropriate starting point for total-energy calculations at temperatures beyond melting. For a large range of intermediate temperatures (*i.e.* below the cluster melting point) *bcc* lattice-induced structures appear to be the most stable ones, as is seen in the schematic phase diagram reported below.

A new physical interpretation of the electronic magic numbers, where cluster stability is observed in high-temperature experiments, is also obtained in terms of an enhanced uniformity of calculated electronic charge density for these particularly stable cluster sizes.

The model system and the hamiltonian for total energy calculation are described in detail in Ref. 17. The starting point for any

given cluster size N is to place the ionic cores at regular finite lattice sites. Density functional theory is used and the effective Kohn-Sham potential seen by each electron is approximated by a flat potential well bounded by an infinite wall, the shape of which is, in principle, determined by the position of the outermost atoms of the cluster. The finite lattice is then relaxed in a "rigid" electronic background to get to the ionic structure corresponding to the lowest energy configuration. Only wells of spherical shapes are considered because of practical, calculational requirements. For concreteness, *bcc* (bulk crystalline structure of Na metal above 5 K) and *fcc* (representative of a close-packed structure) lattices truncated by the electron-confining sphere are used as starting-point structures for the clusters. In conformity with the high (spherical) symmetry of the electron environment, truncated lattices of only tetrahedral or higher point-group symmetry are included. The electronic charge outside the jellium sphere, caused by the finiteness of the cluster work-function, is taken into account by placing the effective uniform jellium sphere a "decay-length" $\delta = 0.29a$ inside the electron confining wall[17], where a is the bulk lattice-constant for Na. The energy involved in the distortion of the electronic charge density at and around the ionic sites is calculated in the first-order perturbation of the local pseudopotential; exchange and correlation effects are handled in the local-density approximation (LDA) scheme[18]. The total energy consists of electronic kinetic energy, exchange-correlation energy, the first-order pseudopotential contribution, and the electrostatic energy. The last contribution is a sum of three terms: the electron-electron Coulomb repulsion, the ion-ion Madelung energy, and the electron-ion

Coulomb attraction. For any given cluster size, the spherical shells of atoms are radially and angularly relaxed to reach the lowest energy configuration compatible with the chosen spherical symmetry of the electronic charge.

In Ref. 17 it is shown that when a zero-temperature total energy hull is constructed for all cluster sizes N, the nature of the most stable clusters, *i.e.*, those **on** the hull, changes as a function of N. For smaller sizes the clusters on the hull owe their stability to quantal effects and correspond to complete electronic angular momentum shells. Such clusters comprise a series of so-called electronic magic numbers. The larger clusters, on the other hand, always belong to an *fcc* cluster truncated by the electron-confining sphere, with complete spherical shells of atoms. Such clusters form a series of geometrically-closed *fcc* lattice-induced numbers. The largest of the electronic magic-number series and the smallest of the *fcc* series on the total-energy hull are 58 and 141 respectively, *i.e.*,the dividing line between the two series is approximately at $N \sim 100$. Calculations for $N > 200$ show that the electronic magic numbers are always less stable, at $T = 0$, than the structures with complete atomic shells. Figure 1 shows the total energy hull, at $T = 0$, of the lattice-induced geometrically-closed structures only. All clusters on this hull (solid line) are found to belong to an *fcc* (close-packed) series. In view of the finite-temperature effects discussed below, a separate hull (dashed line) is also drawn for the *bcc* series. Some of the clusters very close to the hulls in energy are also shown. Fits to the two hulls (at T=0) as a function of cluster size N in the asymptotic form[19] are given by:

$$E_{fcc}\ [Ry/atom] = -0.45804 + 0.10486\ n + 0.22905\ n^2\ , \quad (1)$$

$$E_{bcc}\ [Ry/atom] = -0.45770 + 0.10516\ n + 0.33005\ n^2\ , \quad (2)$$

where $n = N^{-1/3}$, and the results for total energy per atom in the bulk ($n=0$) *fcc* and *bcc* crystalline phases of Na have been used[18,20].

In order to obtain the amplitude of lattice vibrations at arbitrary temperatures the vibrational frequency spectrum is approximated by the angular modes of oscillation of the complete spherical shells of atoms. The melting point of a cluster is determined by applying the Lindemann criterion to this shear mode, *i.e.*, to the angular oscillation of an atom on the outermost shell: the lattice melts if the amplitude of such oscillations relative to the layer below is 10% or more of the distance to the nearest neighbor. All other modes (*e.g.*, radial) or displacements (*e.g.*, inner shells) are stiffer, corresponding to smaller displacements and not contributing substantially to the melting of the cluster[21]. The melting temperature T_M thus calculated for several cluster sizes is $T_M = 0$ for $N < 65$, *i.e.*, the melting is produced by the zero-point vibrations; T_M increases sharply between $N \sim 65$ and $N \sim 200$. For larger N it rises slowly toward the bulk value of $T_M = 372$ K, with a few oscillations. Figure 2 shows an interpolated melting curve (with the oscillations removed) as the lower bound of the phase termed "jellium". Physically, the higher polarizability of smaller clusters[2] implies larger screening, lower oscillation frequencies, and larger lattice vibrations at a given temperature: hence lower melting points. For $N < 65$, the zero-point motion of the ionic

cores is large enough to cause lattice melting, and jellium becomes a good model even at T=0. For $N > 65$, however, the stability at the electronic magic numbers predicted from SJBM calculations should be observed only at temperatures above the melting curve. In the experiments of Ref. 4, the cluster temperatures have been estimated to be ~ 400-500 K, clearly above the melting curve of Fig. 2. Another important feature of Fig.2 is the existence of a large region just below the melting curve where the geometrically-closed *bcc* lattice-induced structures become energetically favorable. This result is in agreement with the Landau theory of solidification[22,23]. The curve separating the *bcc* and *fcc* phases is obtained on the assumption that the difference in entropy per atom between the bulk *bcc* and *fcc* phases is insensitive to temperature and cluster-size dependence. The entropy scale is set by the experimental result that bulk Na has a martensitic transformation from *hcp* to *bcc* at $T \sim 5$ K and that the *hcp* and *fcc* are very close in energy. Therefore this *fcc-bcc* crossover temperature as a function of $n = N^{-1/3}$ is given by:

$$T_{cross\text{-}over}(n) = \frac{E_{bcc}(n) - E_{fcc}(n)}{E_{bcc}(0) - E_{fcc}(0)} \cdot 5 \text{ K} \qquad (3)$$

where $E_{bcc}(n)$ and $E_{fcc}(n)$ are given by Eqns. (1) and (2) respectively.

The existence of the *bcc* phase is well supported by the experimental results of Ref. 3, where the cluster temperatures are lower than those of Ref. 4, presumably close to the melting curve of Fig. 2. The maxima in the abundance spectrum of Ref. 3, although

interpreted as electronic magic numbers, are all consistently shifted away from the magic numbers of Ref. 4 towards the *bcc* magic numbers of the present calculation, *i.e.* those on the dashed hull of Fig. 1. Also the lower temperature data exhibit local stability at perhaps other types of geometrically closed structures not considered here.

A new physical interpretation of the experimentally observed electronic magic numbers is obtained by plotting the quantity,

$$\Delta\rho = \underset{\langle\rho\rangle}{\text{Min}} \int |\rho(r)-\langle\rho\rangle| \, 4\pi r^2 dr \qquad (4)$$

as a function of cluster size between 200 and 800 for N with complete electronic angular-momentum shells (see Fig.3). In (4) above, $\rho(r)$ is the electronic number density normalized in terms of the uniform jellium density; $\langle\rho\rangle$ is a constant density that minimizes $\Delta\rho$. If a hull for $\Delta\rho$ is constructed, one obtains a series of cluster sizes at which the electronic charge density is more uniform. These numbers, shown in Fig. 3 are exactly the ones identified as the electronic magic numbers in uniform SJBM calculations[3,4]. Physically, uniform jellium does the most efficient job of electrostatic charge cancellation in these particular clusters, with a lowering of the electrostatic energy and enhancement of cluster stability. This result lends a strong support to the notion that these experimentally observed jellium clusters at high temperatures are liquid clusters, where ionic motion screens out the electronic charge density substantially.

The authors would like to thank S. Bjørnholm for valuable

discussions. This research was supported, at the Lawrence Berkeley Laboratory, by the Office of Energy Research, Office of Basic Energy Sciences, Materials Research Division, U.S. Department of Energy, under Contract No. DE-AC03-76-SF00098.

References

1. W. D. Knight, K. Clemenger, W. A. de Heer, W. A. Saunders, M. Y. Chou, and M. L. Cohen, *Phys. Rev. Lett.* **52**, 2141 (1984).

2. For a detailed review and other references for earlier work, see W. A. de Heer, W. D. Knight, M. Y. Chou, and M. L. Cohen, in *Solid State Physics*, edited by H. Ehrenreich, F. Seitz, and D. Turnbull (Academic, New York, 1987), vol. **40**, pp. 93-181.

3. H. Göhlich, T. Lange, T. Bergmann, and T. P. Martin, *Phys. Rev. Lett.* **65**, 748 (1990); *Mod. Phys. Lett.* **5**, 101 (1991); *Z. Phys. D* **19**, 117 (1991).

4. S. Bjørnholm, J. Borggreen, O. Echt, K. Hansen, J. Pedersen, and H. D. Rasmussen, *Phys. Rev. Lett.* **65**, 1627 (1990); *Z. Phys. D* **19**, 47 (1991).

5. T. P. Martin, T. Bergmann, H. Göhlich, and T. Lange, *Chem. Phys. Lett.* **172**, 209 (1990), *Z. Phys. D* **19**, 25 (1991).

6. M. L. Cohen, M. Y. Chou, W. D. Knight, and W. A. de Heer, *J. Phys. Chem. Solids* **91**, 3141 (1987).

7. W. Ekardt, *Phys. Rev. B* **29**, 1558 (1984).

8. T. Lange, H. Göhlich, T. Bergmann, and T. P. Martin, *Z. Phys. D* **19**, 113 (1991).

9. T. Bergmann, and T. P. Martin, *J. Chem. Phys.* **90**, 2848 (1989).

10. H. Nishioka, K. Hansen, and B. R. Mottelson, *Phys. Rev. B* **42**, 9377 (1990).

11. R. Car, and M. Parinello, *Phys. Rev. Lett.* **55**, 2471 (1985).

12. P. Ballone, W. Andreoni, R. Car, and M. Parinello, *Europhys. Lett.* **8**, 73 (1989).

13 R. Kawai, J. H. Weare, *Phys. Rev. Lett.* **65**, 80 (1990).

14. O. Sugino, and H. Kamimura, *Phys. Rev. Lett.* **65**, 2696 (1990).

15. O. B. Christensen, K. W. Jacobsen, J. K. Nørskov, and M. Manninen, *Phys. Rev. Lett.* **66**, 2219 (1991).

16. J. Y. Yi, J. O. Dirk, and J. Bernholc, *Phys. Rev. Lett.* **67**, 1594 (1991).

17. A. Maiti, and L. M. Falicov, *Phys. Rev. A* **44**, 4442 (1991).

18. E. G. Brovman, Y. Kagan, and A. Kholas, *Fiz. Tverd. Tela* **12**, 1001 (1970) [*Sov. Phys. Solid State* **12**, 786 (1970)].

19. E. Engel, and J. P. Perdew, *Phys. Rev. B* **43**, 1331 (1991).

20. W. A. Harrison, *Pseudopotentials in the theory of metals*, (Benjamin, New York, 1966), p. 193.

21. The temperature effects on the electronic structure -- considered by M. Brack, O. Genzken, and K. Hansen, *Z. Phys. D* **19**, 51 (1991) and by U. Gupta, and A. K. Rajagopal, *Phys. Rep.* **87**, 259 (1982) -- are considerably smaller than those studied here, and therefore not included.

22. S. Alexander, and J. McTague, *Phys. Rev. Lett.* **41**, 702 (1978).

23. Icosahedral-symmetry structures, which could have a lower free energy near the melting curve (Ref. 22), because of the considerable faceting do not fit in a spherical-charge scheme. It is therefore not considered here. For cluster sizes $N > 1000$, however, faceted structures are known to become important, and over an intermediate range of cluster sizes and a given range of temperatures, they should become stable. These icosahedral structures, which exist only for $N > 1000$, have probably been observed experimentally (Ref. 5). There should be therefore modifications in the phase diagram for temperatures close to T_M and for $N > 1000$. The absence of an icosahedral phase for $N < 1000$ is supported by experiments (Ref. 3) and by molecular dynamics (Ref. 16) simulations on Al.

Figure captions

Fig. 1. Total energy hull at $T = 0$ (solid line) for the geometrically closed lattice-induced structures for cluster sizes $200 < N < 800$. Only *fcc* lattice-induced structures denoted by black squares are on this hull. The most stable geometrically closed *bcc* clusters (denoted by '+'s) and the corresponding hull (dashed line) are indicated. Clusters very close to the hulls are also shown.

Fig. 2. Temperature-size phase diagram for clusters of size $N < 1000$.

Fig. 3. Non-uniformity in electron density $\Delta\rho$ (defined in the text), in arbitrary units, for clusters with complete electronic angular-momentum shells. Cluster sizes on the stability hull are indicated by the proper number labels.

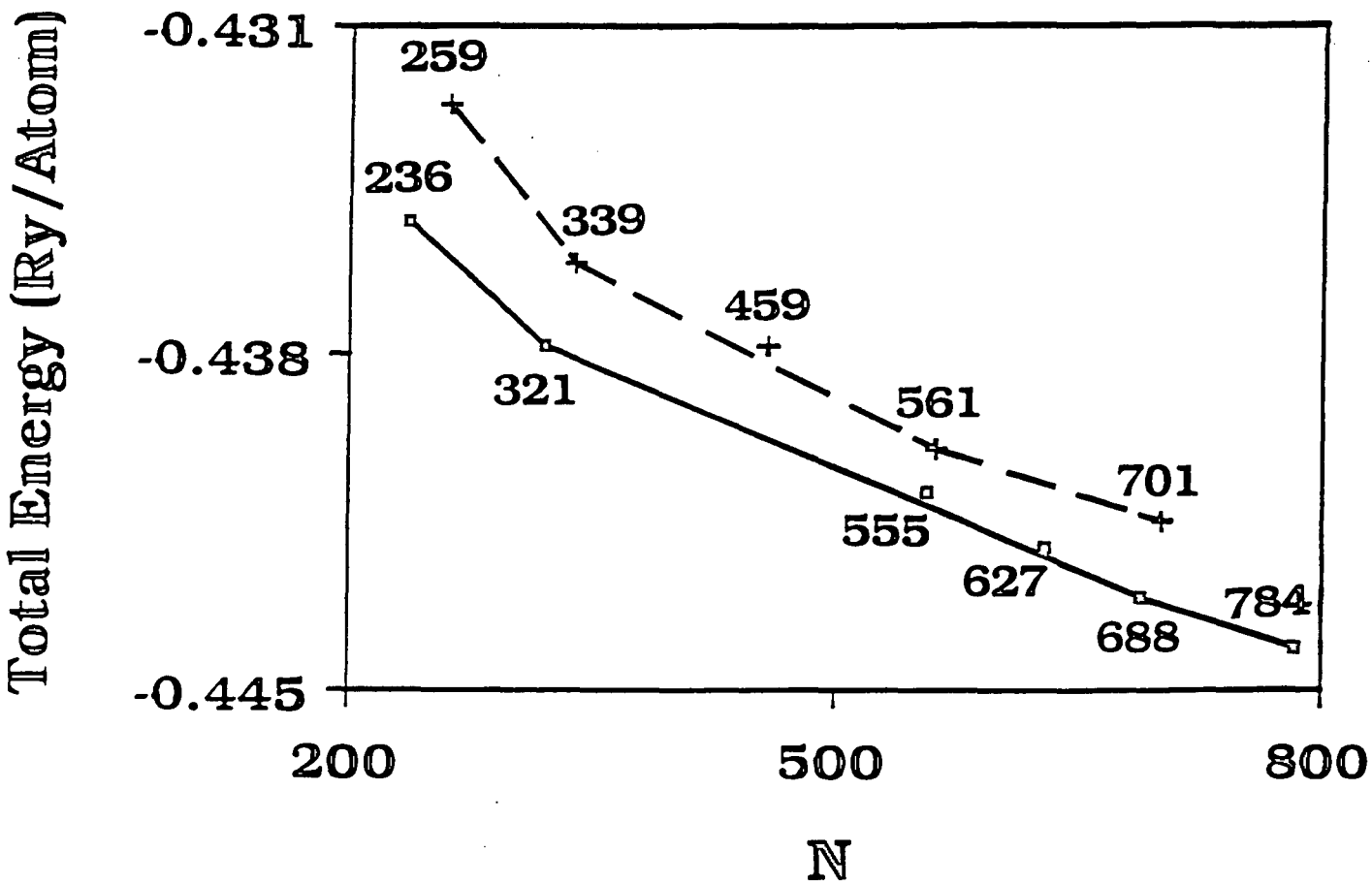
Total Energy (Ry/Atom)
-0.431
-0.438
-0.445
200
500
800
N
259
236
339
459
321
561
701
555
627
784
688

FIGURE 1

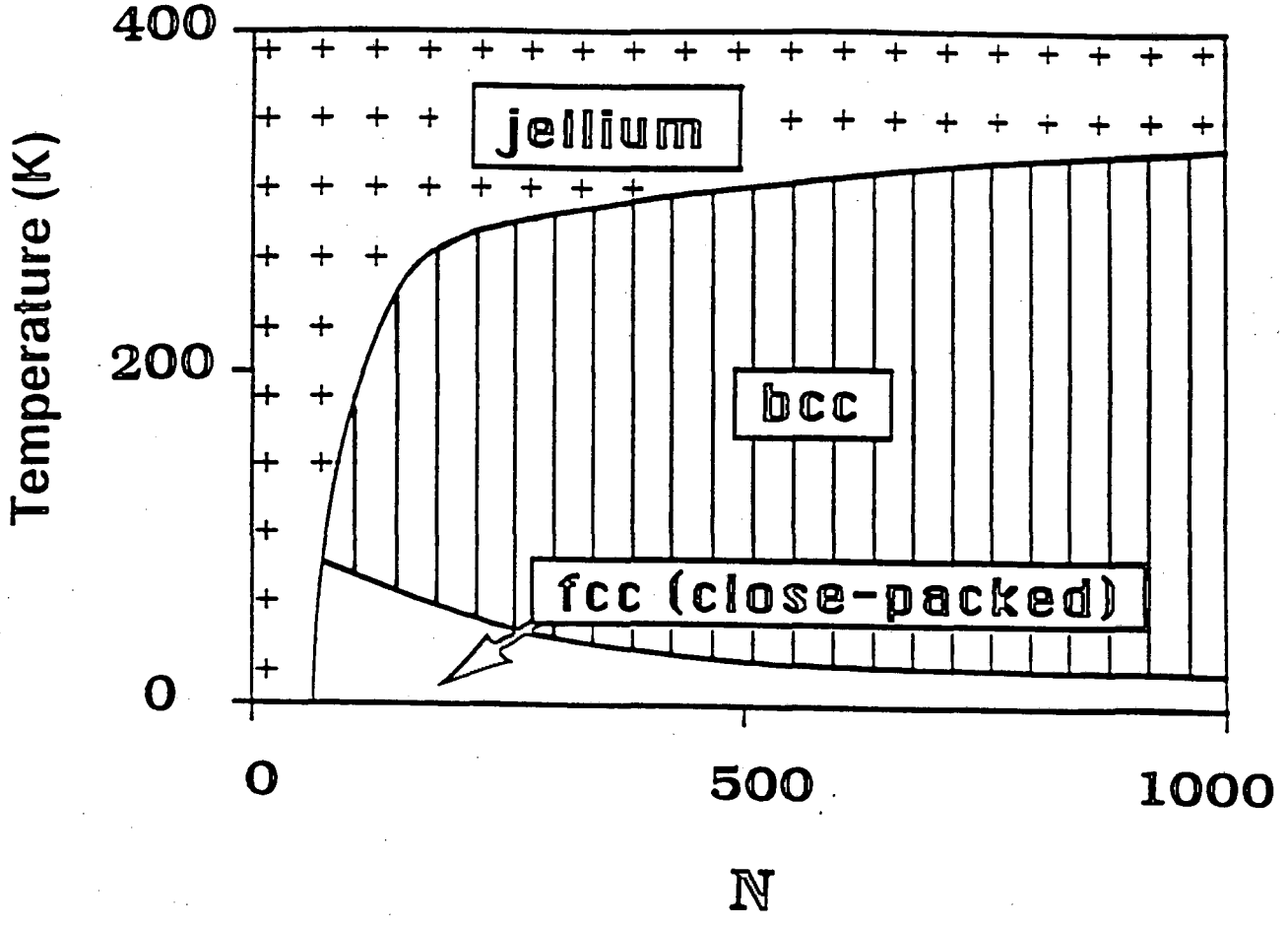
400
200
0
Temperature (K)
jellium
bcc
fcc (close-packed)
0
500
1000
N

FIGURE 2

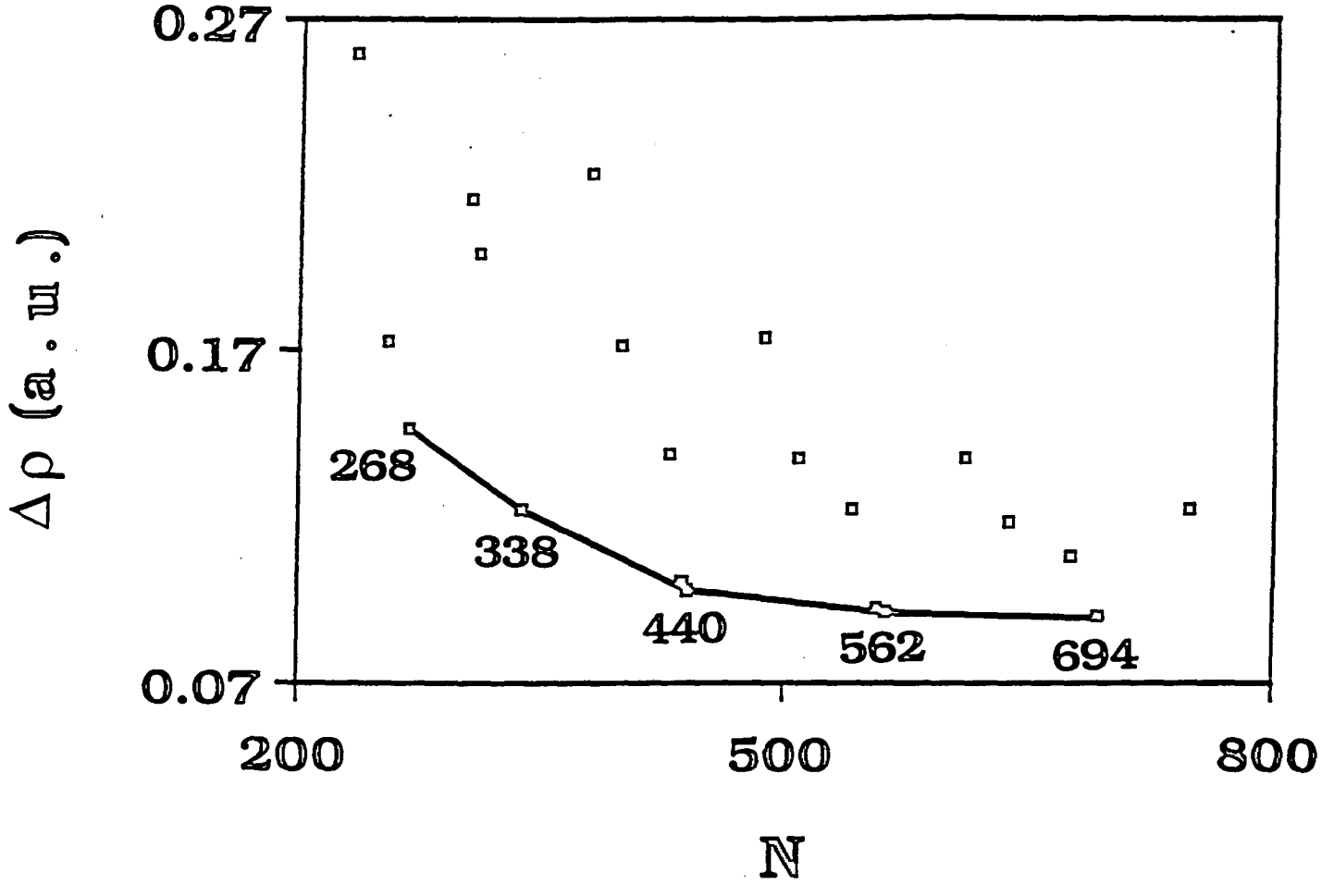

FIGURE 3

LAWRENCE BERKELEY LABORATORY
UNIVERSITY OF CALIFORNIA
INFORMATION RESOURCES DEPARTMENT
BERKELEY, CALIFORNIA 94720